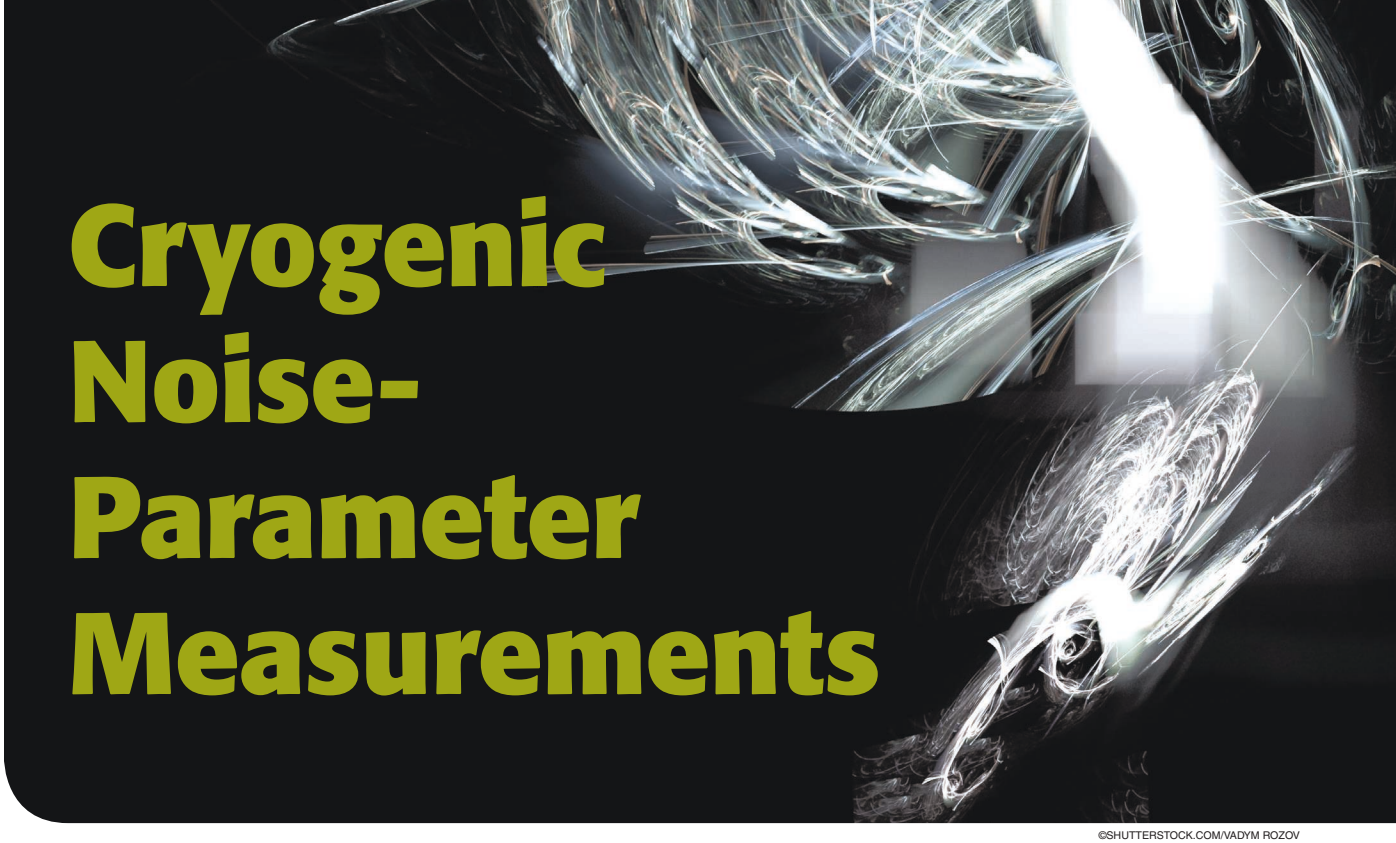

Cryogenic Noise-Parameter Measurements

©SHUTTERSTOCK.COM/VADYM ROZOV

Alexander Sheldon, Leonid Belostotski, Hamdi Mani, Christopher E. Groppi, and Karl F. Warnick

Since the conception of radio astronomy [1], researchers have been striving to develop a "zero-noise" broadband receiver. Although this goal has remained elusive, the pursuit of it has led to numerous low-noise circuit innovations [2], [3]. Perhaps the most notable of these innovations are cryogenic low-noise amplifiers (cryo-LNAs) [3]–[6] as this technology has been able to achieve the lowest noise levels to date. While references to cryogenic amplifiers in the literature date back to the early 1950s [7], they are still a subject of much interest among researchers. Cryo-LNAs were initially conceived of to address challenges in the fields of space exploration [8], [9] and radio astronomy [10]. More recently, researchers in other fields have become interested in "zero-noise" receivers, making this a topic of widespread interest among RF and microwave engineers.

Over the last several decades, cryo-LNAs have been incorporated into radio astronomy telescopes to enhance their sensitivity [3]–[6]. While conventional telescopes are designed to have a single receiver for each antenna, antenna arrays use multiple receivers to increase the survey speeds [11], [12]. Given the interest in faster surveys, antenna arrays are expanding considerably the range of applications for cryo-LNAs. Cryo-LNAs are also required for telescopes employing highly sensitive microwave kinetic inductance detectors [13], [14]. In addition to their radio astronomy applications, cryo-LNAs are also commonly utilized in high-performance communication links, such as those used in satellites [15]. More recently, the development of quantum computers has drastically increased interest in utilizing cryo-LNAs to move room-temperature electronics closer to qubits to reduce the thermal load in dilution cryostats, which arises because of the interconnects to

Alexander Sheldon (awsheldo@ucalgary.ca) and Leonid Belostotski (lbelosto@ucalgary.ca) are with the University of Calgary, Calgary, Alberta, T2N 1N4, Canada. Hamdi Mani (hamdi.mani@asu.edu) and Christopher E. Groppi (christopher.groppi@asu.edu) are with Arizona State University, Tempe, Arizona, 85281, USA. Karl F. Warnick (warnick@ee.byu.edu) is with Brigham Young University, Provo, Utah, 84602, USA.

Digital Object Identifier 10.1109/MMM.2021.3078027

Date of current version: 8 July 2021

room-temperature electronics [16]–[20]. This increased interest in cryo-LNAs is reflected in the growing number of related publications that have been appearing in the literature, as illustrated in Figures 1 and 2.

The Importance of Cryo-LNAs

For Radio Telescopes

Maximizing radio telescope sensitivity allows astronomers and astrophysicists to look deeper into space and further back in time. A radio telescope sensitivity is proportional to $A_{\text{eff}}/T_{\text{sys}}$, where A_{eff} is the effective collecting area of the telescope and T_{sys} is the system noise temperature. Given the significant physical and budgetary constraints associated with increasing A_{eff}, efforts to increase sensitivity have primarily concentrated on decreasing T_{sys}. However, the system noise temperature, T_{sys}, is limited by the front-end LNA noise temperature, T_{LNA}. Despite efforts to reduce T_{LNA} without resorting to cryogenic cooling for telescopes with a large number of receivers [22]–[28], cryogenic cooling is still primarily used [3], [6], [29]–[32]. Although there are a number of well-documented design methods that use LNA noise parameters to reduce T_{LNA}, they are difficult to implement at cryogenic temperatures because of the limited availability of cryogenic-noise-parameter measurement equipment. This is an important limitation as the noise parameters of the devices at cryogenic temperatures and various biases are required for optimum designs.

For Quantum Computers

The advent of spin-electron and transmon qubits [33], [34] has initiated a push to develop fully integrated quantum processors in silicon technologies [16]–[19]. To avoid thermal disturbances and decoherence, quantum processors are designed to operate at temperatures below 25 mK; however, they are still prone to errors and may require many hundreds of qubits for each error-corrected qubit [16], [35]. Such large numbers of qubits will require highly integrated, cryogenically cooled readout and control circuitry located near the qubit devices as this will help to reduce thermal load from the interconnects on dilution cryostats and also minimize readout noise [16]–[19]. Since this readout circuitry contains low-power and very-low-noise cryo-LNAs, these LNAs must be carefully modeled [36] and verified to ensure the best performance possible.

Cryogenic Noise-Parameter Measurements

Noise parameters model the effect of signal-source impedance on the circuit noise temperature. Unlike noise temperatures/factors, which pertain only to a certain signal-source impedance, noise parameters provide the most comprehensive picture of LNA noise properties and insights into the reduction of LNA noise.

The development of quantum computers has drastically increased interest in utilizing cryo-LNAs to move room-temperature electronics closer to qubits to reduce the thermal load in dilution cryostats.

Thus, their measurement is critical for radio astronomy, quantum computing, and other applications. Noise parameters include the minimum noise temperature, T_{min}, the noise resistance, R_n, and the optimum complex reflection coefficient or admittance, Γ_{opt} or Y_{opt}, for minimum noise. While noise-parameter measurements have been utilized for many decades [37], the measurement and use of cryogenic noise parameters are still relatively uncommon, and only a few methods have been previously described in the literature (e.g., [5] and [38]–[45]). This article reviews the cryo-LNA noise-parameter measurement techniques that have been reported, and it highlights a recent method based

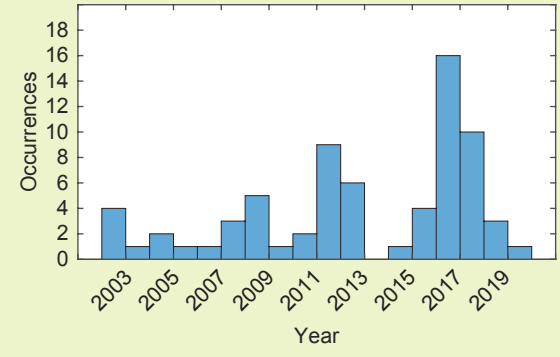

Figure 1. *A histogram of the cryo-LNAs published since 2000 [21].*

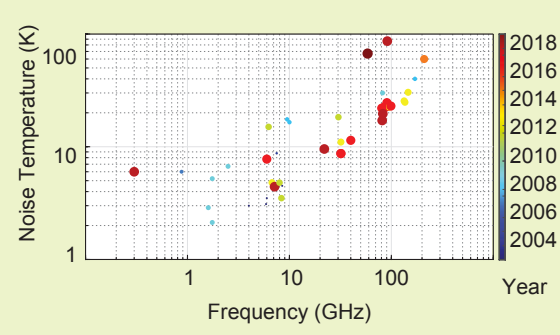

Figure 2. *Noise temperature versus frequency of cryo-LNAs published since 2000 [21]. The brighter markers of larger size indicate newer designs.*

Acquiring noise measurements at cryogenic temperatures takes substantially longer than at room temperatures because of the need for lengthy cooling cycles between measurements.

on a commercial impedance generator. To this end, we present the measurement results of a cryo-LNA that will be used in the Advanced L-band Phased Array Camera for Arecibo (ALPACA) [11], which is currently being developed at Cornell University, Brigham Young University, and the Arecibo Observatory.

Noise Measurement at Cryogenic Temperatures

Before reviewing the various methods of measuring noise parameters at cryogenic temperatures, it would be useful to provide an overview of the unique difficulties associated with measuring the scattering parameters (S-parameters) and noise of a device under test (DUT) at cryogenic temperatures. These difficulties mainly arise because of differences in the DUT and measurement equipment ambient temperatures, the lengthy DUT cooling cycles, and the inability to reconfigure the measurement system without warming it to room temperature. Addressing these difficulties is critical as they can all limit the accuracy and feasibility of the measurements.

Measurement Time

Acquiring noise measurements at cryogenic temperatures takes substantially longer than at room temperatures because of the need for lengthy cooling cycles between measurements. Indeed, it is not uncommon for a typical cryogenic noise-parameter measurement to take three to five days. Thus, the number of cooling cycles is a significant factor when choosing a measurement method. Aside from cooling, noise-power spectrum measurements and the amount of noise averaging may also significantly influence the measurement duration at both cryogenic and room temperatures.

DUT Interconnects

In a noise-parameter measurement system, various passive elements are used to interface the DUT to the measurement equipment. However, these elements are not part of the DUT and should be de-embedded from the measurements. De-embedding passive elements under thermal equilibrium requires a knowledge of their S-parameters (or available gain) and physical temperatures. By contrast, de-embedding passive elements that experience temperature gradients and that are not under thermal equilibrium is more troublesome. These elements are typically associated with the coaxial interconnects that are required to interface the DUT inside of the cryostat with the room-temperature measurement equipment outside of the cryostat. These interconnects are commonly made from stainless steel coaxial cables to reduce their thermal conductivity and thermal gradients, but this comes at the cost of higher loss and a higher noise contribution. Since these interconnects are not at thermal equilibrium, a knowledge of their available gains and physical temperatures is inadequate for estimating their noise contribution. The bounds on the noise temperature, T_{ic}, of an interconnect having an available gain $G_{\text{ic}}^{\text{av}}$ are expressed as

$$T_{\text{cryo}}\left(\frac{1}{G_{\text{ic}}^{\text{av}}}-1\right)\le T_{\text{ic}}\le T_{\text{amb}}\left(\frac{1}{G_{\text{ic}}^{\text{av}}}-1\right) \tag{1}$$

where T_{amb} is the ambient temperature and T_{cryo} is the temperature inside the cryostat. While $\left|G_{\text{ic}}^{\text{av}}\right|=1$ is desirable, coaxial cables with a high available gain also have low thermal resistance, which leads to higher temperatures inside the cryostat. Most of the noise-parameter measurement methods reviewed in this article incorporate different approaches to either eliminating the need for interconnects, particularly the interconnect at the DUT input, or modeling them and correcting for their noise.

Thermal Loading

The power consumption inside the cryostat and the bias and control leads contribute to thermal loading and increased temperature of the DUT. While the use of multiple temperature sensors would provide a good picture of the temperatures at different locations within the cryostat, incorporating more than a couple necessitates more leads, which may increase the temperature of the parts inside the cryostat. Thus, the use of multiple sensors requires special considerations.

Noise-Temperature Measurements

Noise-parameter measurements rely on noise-temperature (noise-figure) measurements. Typically, noise-temperature measurements of a room-temperature DUT are conducted using the *Y*-factor method [46] or the cold method (see "An Introduction to Noise-Temperature Measurements"), requiring a noise source that is connected directly to the DUT input and serves as a calibrated noise-temperature standard. Commonly, the manufacturer-supplied excess noise ratio (ENR) specifies the noise-source noise temperature (see "The Definition of ENR"). Unfortunately, this

An Introduction to Noise-Temperature Measurements

Often circuits need to be measured to characterize the amount of noise they add to incoming signals and the effect of the noise on the signal-to-noise ratio (SNR). The degradation of output SNR ($\mathrm{SNR_{out}}$) relative to the input SNR ($\mathrm{SNR_{in}}$) is denoted as the noise factor $F \equiv \mathrm{SNR_{in}}/\mathrm{SNR_{out}}$. Depending on the application, the noise factor is also represented as the noise figure, $\mathrm{NF} = 10\log_{10}(F)$, or as the noise temperature, $T = T_0(F-1)$, where $T_0 = 290\,\mathrm{K}$ is the reference temperature. The noise temperature is a useful parameter for very-low-noise amplifiers (or cryo-LNAs) because the units of noise factors and noise figures tend to obscure variations in very-low-noise temperatures, where even a difference of 1 K can be significant. Conventional measurements of noise factors include the *Y*-factor method and the cold method [S1].

To measure the noise factor with the *Y*-factor method, a noise source is connected to the input of the DUT, and a calibrated receiver is connected at the output of the DUT. As the noise source is switched from on and off, it produces noise power densities of $N_\mathrm{h} = kT_\mathrm{h}$ and $N_\mathrm{c} = kT_\mathrm{c}$, respectively, where T_h and T_c are the noise temperatures of the noise source and k is Boltzmann's constant. The receiver measures the DUT output noise-power spectral densities N_hot and N_cold corresponding to the noise-source states. The noise temperature and available gain of the linear DUT are calculated as

$$T_\mathrm{DUT} = \frac{T_\mathrm{h} + YT_\mathrm{c}}{Y-1} \tag{S1}$$

and

$$G_\mathrm{av} = \frac{N_\mathrm{hot} - N_\mathrm{cold}}{N_\mathrm{h} - N_\mathrm{c}}, \tag{S2}$$

where

$$Y \equiv \frac{N_\mathrm{hot}}{N_\mathrm{cold}}. \tag{S3}$$

To measure the noise factor with the cold-source method, first the S-parameters of the DUT are measured with a vector network analyzer (VNA), and the transducer gain, G_T, is calculated. Then a 50-Ω termination is connected to the input of the DUT, and a calibrated receiver is connected at its output to measure the output noise power spectral density, N_out. The noise temperature is then found from

$$T_\mathrm{DUT} = \frac{N_\mathrm{out}}{kG_T} - T_\mathrm{term}, \tag{S4}$$

where T_term is the physical temperature of the termination.

References

[S1] M. Rudolph, P. Heymann, and H. Boss, "Impact of receiver bandwidth and nonlinearity on noise measurement methods [application note]," *IEEE Microw. Mag.*, vol. 11, no. 6, pp. 110–121, 2010. doi: 10.1109/MMM.2010.937715.

The Definition of ENR

There is an inconsistency when it comes to the definition of ENR. Some authors define ENR as $\mathrm{ENR} = (T_\mathrm{h}^\mathrm{ns} - T_0)/T_0$, where T_h^ns is the temperature of the noise source in the on (hot) state, and $T_0 = 290\,\mathrm{K}$, whereas some definitions use $\mathrm{ENR} = (T_\mathrm{h}^\mathrm{ns} - T_\mathrm{c}^\mathrm{ns})/T_0$. The former definition does not explicitly take into account the effect of ambient temperature variations on T_h^ns. While either definition can be used, in this article and all analyses within, the latter definition is adopted as it is consistent with both the recommended definition and the one used in commercial noise-figure analyzers [S2], [S3], and it is the ENR supplied with the noise source used in measurements.

References

[S2] "Agilent fundamentals of RF and microwave noise figure measurements," Agilent Technologies, Inc., Santa Rosa, CA, Application Note 57-1, Oct. 2006.

[S3] L. Belostotski, "A calibration method for RF and microwave noise sources," *IEEE Trans. Microw. Theory Techn.*, vol. 59, no. 1, pp. 178–187, Jan. 2011. doi: 10.1109/TMTT.2010.2086066.

approach is not currently tenable for cryogenic DUTs because of the unavailability of commercial cryogenic noise sources. Aside from developing custom-made noise sources [45], there are two methods (and variants) of measuring cryogenic noise temperatures: the cold-source method [42], [47] and the cold-attenuator method [42], [48].

The Cold-Source Method

A simplified block diagram of the cold-source method is shown in Figure 3. This method requires a measurement of the termination temperature, T_term, and two RF measurements: the S-parameters of the DUT, S_DUT, and the DUT output noise power spectrum, N_out, with the DUT being driven by the termination. N_out is measured

using a calibrated receiver, which can be either a spectrum analyzer, a noise-figure analyzer, or a radiometer, while S_{DUT} is measured using a vector network analyzer (VNA). T_{term} is measured using a diode temperature sensor. The direct implementation of this method requires two cooling cycles to complete the two RF measurements. The use of an RF switch inside the cryostat (Figure 4) enables the measurements to be completed in a single cooling cycle, provided the VNA has been calibrated at the DUT input plane (see "VNA Calibration at Cryogenic Temperatures"). These measured quantities are then used to calculate the noise temperature:

$$T_{DUT} = \frac{N_{out}}{kG_T} - T_{term}, \qquad (2)$$

where N_{out} is expressed in units of watts per Hertz, k is Boltzmann's constant, and G_T is the transducer gain of the DUT, which is calculated from S_{DUT}, Since the uncertainty in N_{out} can be reduced via longer averaging, the accuracy of this noise temperature will largely depend on the accuracy of the measurements of the S-parameters and the termination temperature.

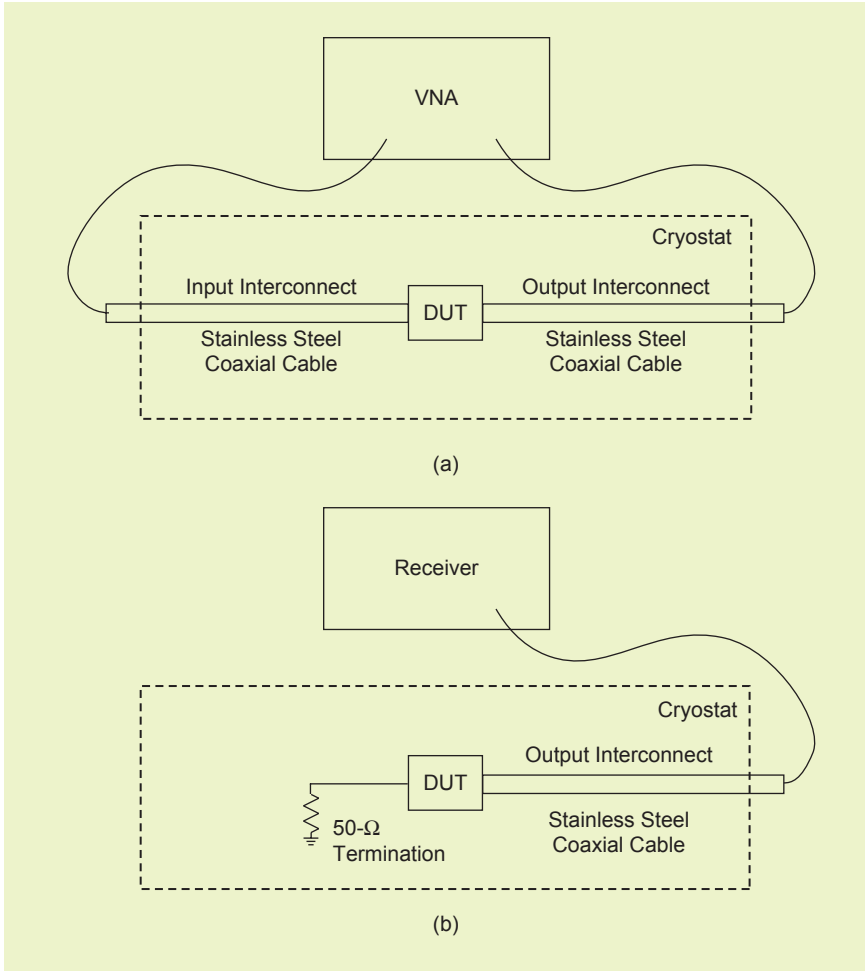

Figure 3. *A block diagram of the cold-source method: (a) S-parameter measurement and (b) noise-power measurement.*

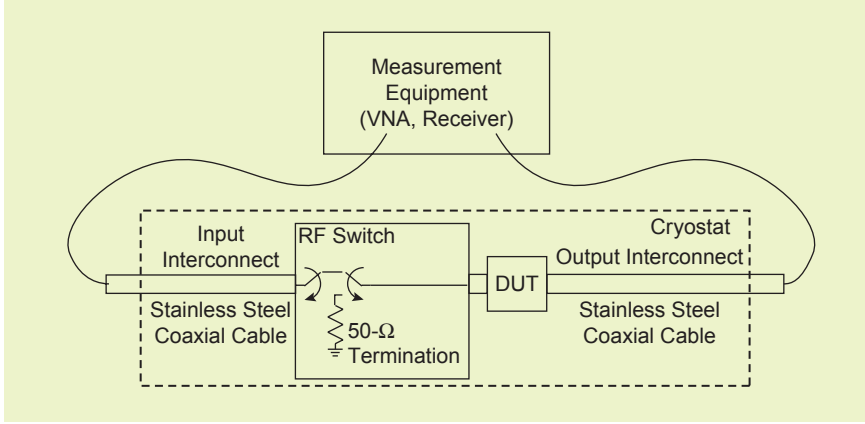

Figure 4. *A block diagram of the cold-source method with a switch. Term.: termination.*

The Cold-Attenuator Method

A block diagram of the required measurement setup is shown in Figure 5. In this method, the DUT is placed in the cryostat with an attenuator at its input, and an interconnect inside the cryostat is connected to a noise source outside the cryostat. The output noise-power spectra, N_{hot} and N_{cold}, are then measured with the noise source in the on (hot) and off (cold) states, respectively. This method enables both of these measurements to be completed in a single cooling cycle and also allows both the DUT noise temperature and the transducer gain to be determined using standard Y-factor noise-measurement procedures [46]. An attenuator is also implemented to reduce the large errors in noise levels at the DUT input caused by uncertainties in the noise-source ENR [49] and the

temperature gradients in the input coaxial cable. The noise temperature of the DUT is found via

$$T_{\mathrm{DUT}} = \frac{T_{\mathrm{h}} - YT_{\mathrm{c}}}{Y-1}, \tag{3}$$

where T_{h} (T_{c}) is the noise temperature at the DUT input with the noise source on (off), and $Y \equiv N_{\mathrm{hot}}/N_{\mathrm{cold}}$ is the Y-factor as measured by the receiver. $\mathrm{T_h}$ and $\mathrm{T_c}$ are functions of the noise source ENR, the gain of the input interconnect, $G_{\mathrm{ic}}^{\mathrm{av}}$, and the available gain of the attenuator, $G_{\mathrm{att}}^{\mathrm{av}}$, are derived as

$$T_{\mathrm{h}} = [(T_{\mathrm{h}}^{\mathrm{ns}} + T_{\mathrm{ic}})G_{\mathrm{ic}}^{\mathrm{av}}]G_{\mathrm{att}}^{\mathrm{av}} + (1 - G_{\mathrm{att}}^{\mathrm{av}})T_{\mathrm{cryo}} \tag{4}$$

and

$$T_{\mathrm{c}} = [(T_{\mathrm{c}}^{\mathrm{ns}} + T_{\mathrm{ic}})G_{\mathrm{ic}}^{\mathrm{av}}]G_{\mathrm{att}}^{\mathrm{av}} + (1 - G_{\mathrm{att}}^{\mathrm{av}})T_{\mathrm{cryo}}, \tag{5}$$

where T_{ic} is the noise temperature of the input interconnect, which is assumed to be at the midpoint of T_{amb} and T_{cryo}. In terms of the noise temperatures, $Y = (T_{\mathrm{h}} + T_{\mathrm{DUT}})/(T_{\mathrm{c}} + T_{\mathrm{DUT}})$ is dependent on the ratio of two noise-power measurements, which is typically accurate. Therefore, in this measurement, the accuracy of the measurement for T_{DUT} depends mainly on the accuracy of the noise-source ENR and the uncertainty in T_{ic}, which is reduced when the attenuator $G_{\mathrm{att}}^{\mathrm{av}}$ is small (i.e., a large attenuator). However, $G_{\mathrm{att}}^{\mathrm{av}}$ cannot be made arbitrarily small, as this would result in $Y \approx 1$ and an increased sensitivity of (3). As such, a 15- to 20-dB attenuator is typically used to make T_{h} comparable to T_{DUT} [42]. In addition to the previous measurements, this method requires a knowledge of the S-parameters of the attenuator and the input interconnect.

Discussion

When a switch is used in the cold-source method, the number of cooling cycles for both methods is the same; however, the cold-source method requires one less noise-power spectrum measurement. In addition, in the cold-source method, the S-parameters of the DUT are determined in the same cooling cycle as the noise measurements. However, by contrast, only the available gain is measured in the cold-attenuator method, with an additional cooling cycle being required for the S-parameter measurement unless a switch is used to bypass the attenuator. Furthermore, the cold-source method does not depend on the estimate of T_{ic} and the noise-source ENR uncertainty. Instead, the accuracy of the cold-source method is reliant on the accurate measurement of the physical temperature of the termination. The advantage of the cold-attenuator method is its reliance on noise-power ratios rather than absolute noise powers. With respect to the calibration procedure, both methods require the same number of cooling cycles because the cold-attenuator method requires the attenuator S-parameters.

VNA Calibration at Cryogenic Temperatures

In theory, a VNA can be calibrated to the ends of the input and output coaxial cables that are located at cryogenic temperatures by using any standard calibration methods (e.g., thru-reflect-line, short-open-load-thru, and so on); however, this calibration process takes a significant amount of time (three to four cooling cycles). Additionally, as open and short standards have different thermal conductivities to the cold head (low conductivity for open and high conductivity for short standards), they may affect the temperature of the coaxial cables and introduce measurement uncertainty. Because of the duration of the cooling cycles, it is more practical to use a two-tier calibration method: the VNA is calibrated to the external coaxial cable RF connectors; then, the S-parameters of the coaxial cables are determined using, for example, a fixture removal measurement, which is available in most modern network analyzers. Consequently, all S-parameter measurements of cryo-LNAs require a postprocessing step of de-embedding the coaxial cables.

Review of Noise-Parameter Measurement Methods

To measure the noise parameters, the noise temperatures of the LNA are measured for at least four different

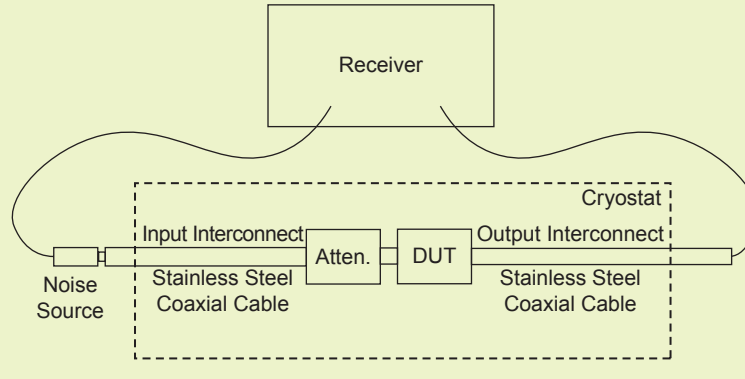

Figure 5. *A block diagram of the cold-attenuator method. Atten.: Attenuator.*

signal-source impedances [50]–[59]. At room temperature, these impedances are commonly generated with mechanical impedance tuners. However, such tuners are much too large to fit in cryostats, and placing them outside the cryostat restricts measurements because of the unknown noise contribution from the cryogenic-to-room-temperature interconnect, whose loss also restricts the attainable impedances. When measuring the noise parameters, there are four unknowns: $T_{\min}$, R_n, $\Re\{\Gamma_{\text{out}}\}$, and $\Im\{\Gamma_{\text{out}}\}$; therefore, at least four measurements are needed. They are described in the following sections.

Calibration

Regardless of the method, the system must be calibrated (see "VNA Calibration at Cryogenic Temperatures"). Since, a cooling cycle is typically required for each such measurement, this process is rather time consuming. However, once the VNA has been calibrated, it is able to retain its calibration for multiple measurement cycles because of the relatively fixed nature of the components in the cryostat.

Additionally, all methods require the calibration of the receiver that is used for the noise-power measurements. This receiver calibration should be performed at the DUT output plane using one of the noise-parameter measurement methods discussed in the subsequent subsections. If the DUT exhibits a large gain, the receiver calibration can be simplified by performing it at room temperature. If the DUT output impedance remains near 50 Ω for different tuner states, the receiver noise temperature can be used instead of its noise parameters.

Impedance Tuner External to Cryostat

A block diagram of the measurement setup required for this method is shown in Figure 6. In this method, a tuner located outside of the cryostat [40], [43], [44] is used to generate a minimum of four impedance states at the DUT input. Noise-power measurements at each tuner state can then be used to extract noise parameters, following, for example, methods detailed in [50]–[59]. However, unlike the case of the room-temperature methods, the noise temperature T_{ic} contributed by the coaxial cable between the tuner and the DUT is unknown and must be de-embedded. Prior studies have employed a few different techniques to account for this noise. In the work of Rolfes et al. [43], the temperature of the interconnect was assumed to be midway between the ambient and cryogenic temperatures, and the interconnect was treated as a passive network at this temperature in thermal equilibrium. Unfortunately, this approach can result in very large uncertainties in measurements. By contrast, in 1994 Escotte et al. [40] used measurements of an additional mismatched passive DUT to determine the noise contribution of this interconnect. More recently, a numerical model of the interconnect noise temperature was proposed by Colangeli et al. [60].

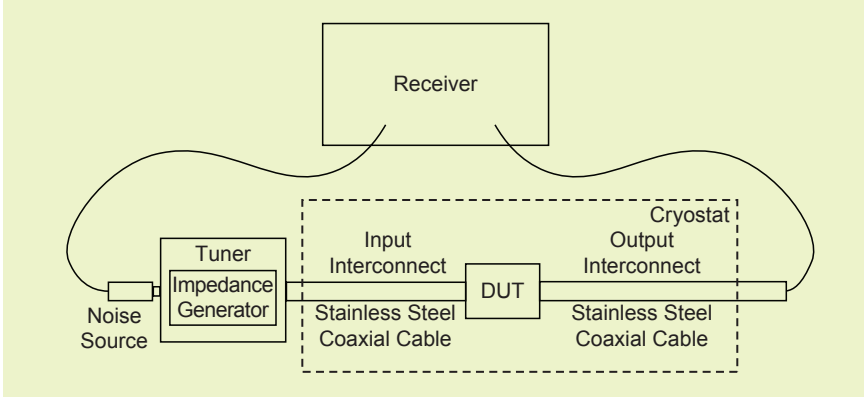

Figure 6. *A system block diagram for measuring cryogenic noise parameters with an impedance tuner at room temperature.*

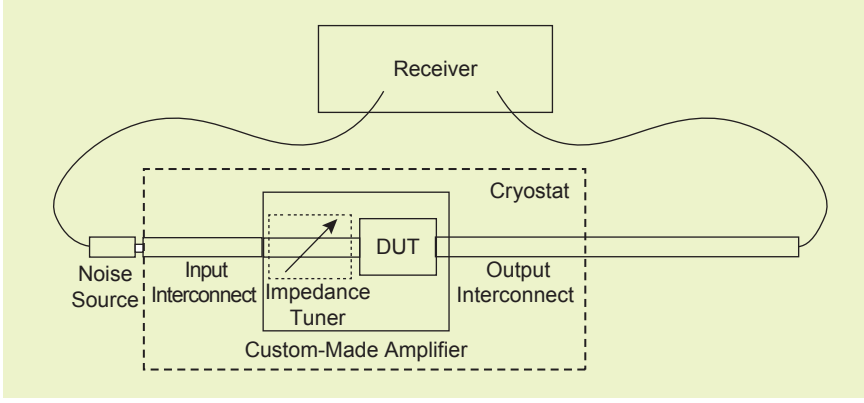

Figure 7. *A system block diagram for measuring cryogenic noise parameters with a custom-made impedance tuner inside the cryostat.*

Impedance Tuner Internal to Cryostat

Earlier works [5], [38], [39] avoided the need for an external impedance tuner by placing a transistor under test within a custom-made amplifier that incorporated a tunable quarter-wave transmission line at the input to the transistor (Figure 7). The impedance of the transmission line was varied using a movable ground plane, thereby generating a set of impedances at the transistor input and permitting the extraction of noise parameters using, for example,

the approach of Lane et al. [50]. The calibration included obtaining a measurement of the S-parameters of the tunable transmission line, with the transistor being replaced by a miniature coaxial probe. Since the noise source was located outside the cryostat in this method, the measurement results were subject to uncertainty because of the unknown noise temperature, T_{ic}. Further, it is not always feasible to develop a custom-made circuit with a tunable transmission line.

The Small-Signal Model Method

Methods of estimating transistor noise parameters using S-parameters, dc measurements, and noise parameters [41] or noise figures [30] have also been proposed. In the work of Laskar et al. [41], an external-to-cryostat tuner was used to extract the noise parameters of the transistor network that included an input interconnect. In this method, the transistor S-parameters and dc I–V curves are measured, and the physical and small-signal element values are determined by fitting these measurements to a circuit model. This method is commonly applied to high-electron mobility transistor (HEMT)-based cryogenic LNAs whose noise behavior is represented using Pospieszalski's noise model [61], wherein the transistor gate noise is modeled by assigning a temperature T_{gate} to the gate resistance, and the drain noise is generated by assigning a temperature T_{drain} to the drain-source transconductance. Here, the measured S-parameters are used to determine all of the values of the small-signal elements, both internal and external to the transistor, using either algebraic techniques or least-squares fitting. Since T_{gate} is approximately equal to the transistor ambient temperature (i.e., $T_{gate} \approx T_{cryo}$ for a cryocooled HEMT), the only unknown, T_{drain}, is found via a 50-Ω noise-temperature (noise-figure) measurement [30]. The small-signal model of the transistor then allows for its noise parameters to be calculated. In the work of Laskar et al. [41], cryogenic noise parameters were predicted based on the extraction of the small-signal model and the noise parameters measured at the external tuner reference plane. Although these methods result in accurate estimates, they require a knowledge of the models for the devices; thus, these approaches are not readily applicable for unknown or new devices or for complex circuits.

Long-Line Method

Hu and Weinreb [42] and Russell and Weinreb [45] presented a noise-parameter measurement method that uses a long transmission line with a rapidly varying impedance. A block diagram of the measurement setup required for this method is shown in Figure 8. In this method, the noise parameters are assumed to be constant over fixed frequency windows. When the DUT input is terminated by a long mismatched transmission line, the DUT signal-source impedance varies rapidly, and consecutive frequency points in fixed windows can be used to solve for the noise parameters. The method presented by Russell and Weinreb [45] uses a cooled device, with the transmission lines and the noise source located in a single cryogenically cooled package. This method requires two noise-power spectrum measurements and three noise-power spectrum measurements for calibration. The noise-parameter measurements and calibration can each be completed in one cooling cycle. Since the required transmission-line length is dependent on the measurement frequency, the low-frequency measurement range is limited by the physical size of the cryostat and the amount of decorrelation experienced by the noise wave propagating through the input transmission lines [62].

Most of the noise-parameter measurement methods reviewed in this article incorporate different approaches to either eliminating the need for interconnects, particularly the interconnect at the DUT input, or modeling them and correcting for their noise.

An Automated Impedance Tuner Internal to the Cryostat

This method uses a commercial solid-state impedance generator [63] that can be placed inside a cryostat,

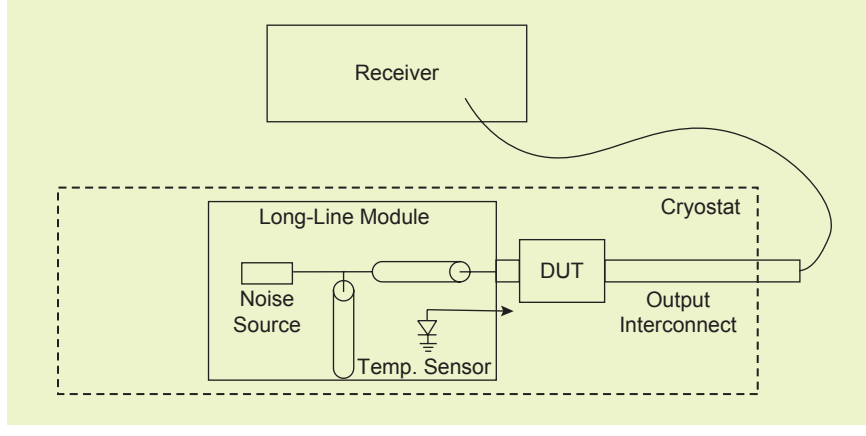

Figure 8. *A block diagram of the long-line method of measuring cryogenic noise parameters. Temp.: Temperature.*

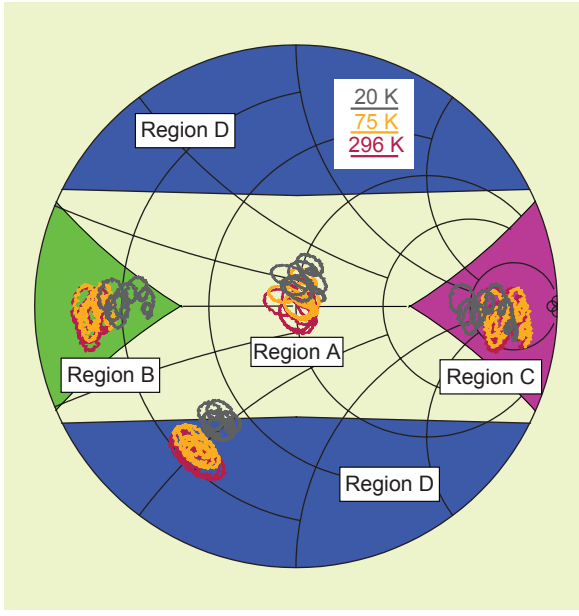

Figure 9. *The tuner impedance constellations in the 1–2-GHz range relative to one of many possible regions that guarantee a diagonally dominant linear system of equations.*

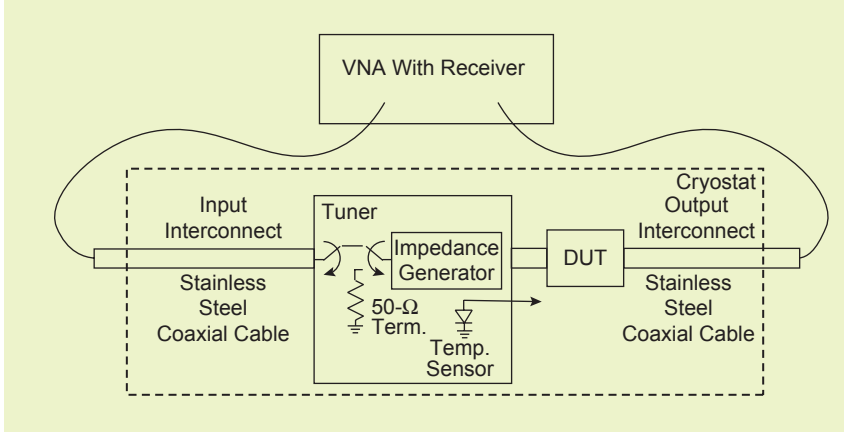

Figure 10. *A block diagram of the measurement system with a tuner inside of the cryostat.*

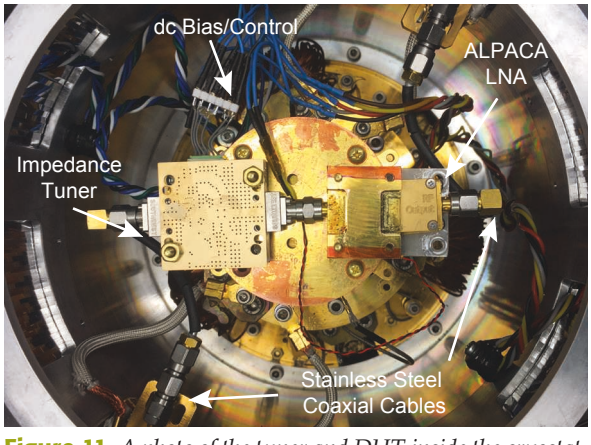

Figure 11. *A photo of the tuner and DUT inside the cryostat.*

enabling the automation of noise-parameter methods. The impedance generator design is such that its realized output impedances follow the impedance patterns identified in the work of Himmelfarb and Belostotski [55]; thereby, with appropriate scaling, it creates diagonally dominant matrices when used with the previously mentioned noise-parameter extraction method [50]. The rest of this article explains a typical measurement, using this method, by way of an example measurement of a radio astronomy cryo-LNA [67].

An Example of Automated Cryogenic Noise-Parameter Measurement

In this example, the impedance generator (tuner) is placed in the cryostat at the input of the LNA. With just four operating states, the tuner realizes impedance constellations that, under a certain transformation, conform to the impedance regions identified by Himmelfarb and Belostotski over the full measurement frequency range, thereby guaranteeing a diagonally dominant linear system of equations [55]. Figure 9 shows the locations of the impedances generated by the tuner at different temperatures over a 1–2-GHz frequency range as well as an example of the impedance regions A, B, C, and D. The shapes of these regions can be adjusted by changing the scaling factors (as shown in Figure 10 of [55]) to accommodate some impedances that appear slightly outside of the symmetrical regions in Figure 9.

A block diagram of the measurement system is shown in Figure 10. Note that this system employs the next-generation version of the impedance generator, which incorporates a temperature sensor and a switch. As discussed previously, the switch reduces the number of required cooling cycles, while the 50-Ω termination and the temperature sensor enable cold-termination noise-temperature measurements. Both the S-parameters and the output noise-power spectra are measured by a VNA with a noise receiver. A photo of the inside of the measurement cryostat is shown in Figure 11.

After calibration, the following measurement steps are taken at each cryogenic temperature:

1) Stabilize the cryostat to the desired temperature, and measure the physical temperature of the termination, T_{term}, with the tuner temperature sensor.
2) Set the tuner to the "THRU" state and measure the S-parameters of the DUT, S_{DUT}.

3) Switch in the cold termination, cycle through the four tuner impedance states (identified as A, B, C, and D), and use the receiver to measure the corresponding output noise power spectra, N_i: $i = A, B, C, D$.

The measurement process is completely automated via a computer running MATLAB and is completed in one cooling cycle.

For each of the tuner-generated admittances, Y_i, the DUT noise temperature, $T_{\mathrm{DUT},i}$, is expressed as

$$T_{\mathrm{DUT},i} = \frac{N_i}{G_{\mathrm{rec}} G^{\mathrm{av}}_{\mathrm{DUT},i}} - \frac{T_{\mathrm{PNA}}}{G^{\mathrm{av}}_i} - T_{\mathrm{term}}, \tag{6}$$

where G_{rec} is the receiver gain obtained during calibration, and $G^{\mathrm{av}}_{\mathrm{DUT},i}$ is the DUT available gain for each state i. Equation (6) is related to the DUT noise parameters by

$$T_{\mathrm{DUT},i} = T_{\mathrm{min}} + T_0 \frac{R_n}{\Re\{Y_{\mathrm{s},i}\}} \left| Y_{\mathrm{s},i} - Y_{\mathrm{opt}} \right|^2, \tag{7}$$

from which the noise parameters, T_{min}, R_n, and Y_{opt} are found [50], [55].

Measurement of ALPACA LNA

The demonstration of the noise-parameter measurement system was carried out using a 1–2-GHz radio astronomy cryo-LNA consuming 14 mW from a 1.6-V supply and designed for the ALPACA array [11]. The measured S-parameters are shown in Figure 12, and the measured noise parameters are shown in Figure 13 with 2σ error bars.

While DUT measurements can be completed in one cooling cycle, each temperature/bias point requires ~10 h, largely because of the receiver bandwidth (0.8 MHz) and the 2,901 frequency points and 256 averages selected for each impedance state. It is possible to decrease the measurement time significantly by increasing the receiver bandwidth, but this increase may introduce measurement errors [62]. Furthermore, fewer frequency points would accelerate measurements until the cooling cycle dominates.

To assess the accuracy of the results, a sensitivity analysis of (6) was conducted to determine each contributor to the overall uncertainty in the noise temperature. The contributors considered in the sensitivity analysis included the measurement equipment uncertainty, which was acquired from the data sheets [64], [65]; the calibration of the temperature sensor $(1\sigma = 0.33\ \mathrm{K})$; and the 1σ uncertainty in S_{coax}, which was estimated at 0.033 dB and 3.33°.

Uncertainties in $T_{\mathrm{DUT},i}$ affect the accuracy of the noise parameters determined via (7). Since the system of equations originating from (7) does not have a closed-form solution for the noise parameters, further analytic analysis of the uncertainty is difficult. Instead, following [54] and [66], MATLAB was used to complete a Monte Carlo analysis. The Monte Carlo simulation was run for 1,000 iterations to determine the uncertainties of the noise parameters, which are shown with 2σ error bars in Figure 13. For noise temperatures and minimum noise temperatures, the typical 1σ uncertainty was $< 10\%$. The measured noise parameters had 1σ measurement uncertainties of $< 10\%$ for T_{LNA} and T_{min}, $< 4\%$ R_n, $< 12\%$ for $|\Gamma_{\mathrm{opt}}|$, and $< 8°$ for $\angle\Gamma_{\mathrm{opt}}$. The measurements demonstrated a shift in Γ_{opt} with temperature, a behavior that was invisible with the noise-temperature measurements only.

The Impact of Cryogenic Noise Parameters on Estimation of ALPACA Performance

This section demonstrates the usefulness of measured noise parameters by using them to update the modeled performance of the ALPACA phased-array feed receiver. During the design of the array antenna feed, a simple set of LNA noise parameters was used. The simple LNA noise parameters, $T_{\mathrm{min}} = 6$ K, $Z_{\mathrm{opt}} = 50\ \Omega$, and $R_n = 0.517\ \Omega$, were based on a design model for the LNA. The previously determined LNA noise parameters at the array design center frequency (1.5 GHz) were $T_{\mathrm{min}} = 8.2$ K, $Z_{\mathrm{opt}} = 30.1 + j10.8\ \Omega$, and $R_n = 0.41\ \Omega$. Relative to the simple LNA noise parameters, the measured LNA has a slightly higher minimum noise temperature and a poorer optimal source reflection coefficient as $|\Gamma_{\mathrm{opt}}|$ ranges from –10 to –15 dB over the 1.3–1.7-GHz ALPACA operating bandwidth.

Figure 14 shows the system noise temperatures modeled for the simple LNA parameters as well as the

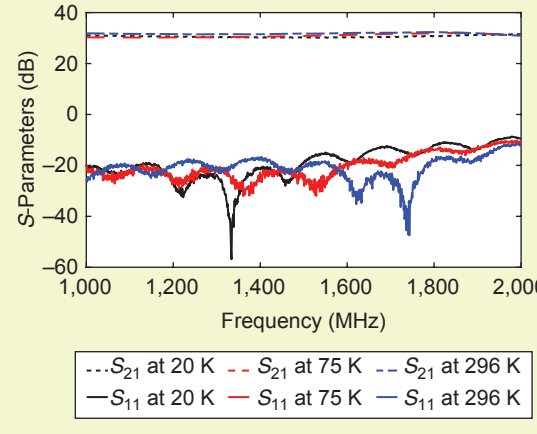

Figure 12. *The S-parameters of the ALPACA LNA at 20, 75, and 296 K.*

Aside from developing custom-made noise sources, there are two methods (and variants) of measuring cryogenic noise temperatures: the cold-source method and the cold-attenuator method.

measured parameters. The system noise temperature budget at 1.5 GHz was $T_{LNA} = 6.7$ K for the LNA noise temperature and 14.8 K for spillover noise, sky noise, and noise due to loss in the front end for the simple LNA noise parameters. For the measured LNA noise parameters, the noise temperature contributed by the LNA increased to 10.2 K. The modeled system noise temperature and spillover noise, which is a function of the LNA noise parameters through the array beam shape, were lower than expected for the ALPACA feed in situ. The model does not include noise resulting from a loss in the vacuum window covering the array or additional spillover noise caused by edge diffraction and other scattering effects. The array was designed using the optimistic noise model, as the objective function of the design was to emphasize aperture efficiency and active impedance matching. The unmodeled noise contributions are largely independent of the array design and were not required in the model used to optimize the design of the ALPACA array feed. From the updated noise budget based on the measured noise parameters, it is concluded that, despite the slightly higher than expected LNA T_{min} and poorer optimal source reflection coefficient, the feed should nearly meet the overall system design target of 25 K system noise temperature when integrated with cryogenic LNAs, particularly given the conservative estimates for spillover and loss noise included in the noise budget.

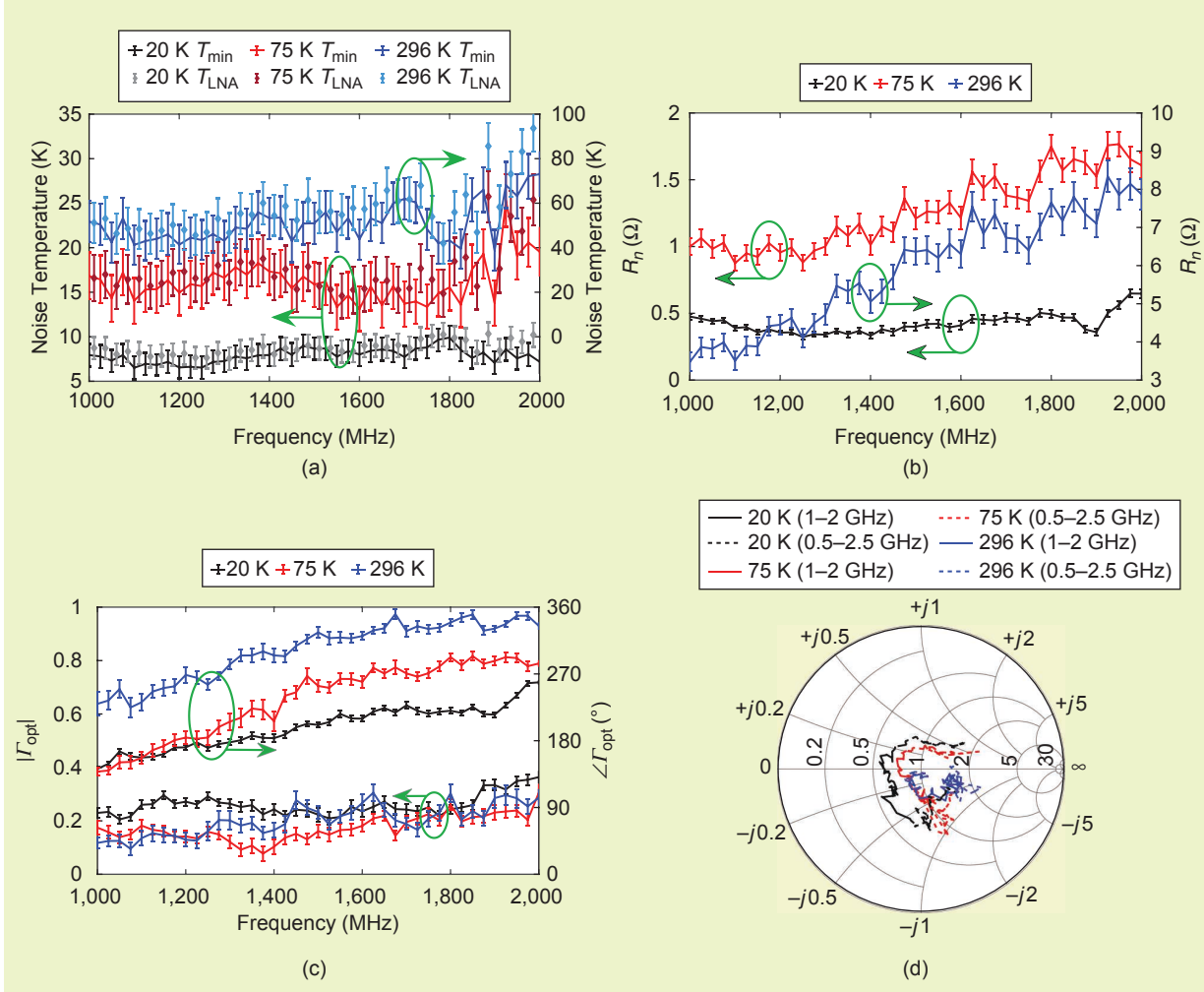

Figure 13. *The measured (a) F_{min} and noise temperatures, (b) R_n, (c) $|\Gamma_{opt}|$, and (d) Γ_{opt} of the ALPACA LNA at 20 K, 75 K, and 296 K with 2σ error bars.*

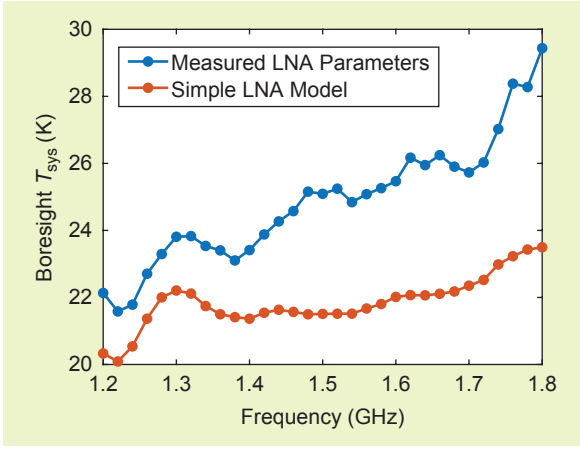

Figure 14. *The modeled ALPACA system noise temperature for the boresight formed beam.*

Conclusions

This article provides a review of cryogenic noise-parameter measurement methods and highlights a recently introduced fully automated measurement solution. Under this new measurement approach, an impedance tuner is placed inside of the cryostat to permit the in situ measurement of noise parameters at different physical temperatures and different biases, thereby enabling the characterization and optimization of cryo-LNAs. An example measurement of ALPACA cryo-LNA noise parameters demonstrated the usefulness of cryogenic noise parameters in estimating the noise performance of the ALPACA antenna array. The characterization method described in this article is intended to support the increasing need for high-quality, low-noise amplifiers in many technological applications.

Acknowledgments

This work was funded by the University of Calgary, the Natural Sciences and Engineering Research Council of Canada (grants RGPIN/03855-2018 and RGPAS/522621-2018), the Canada Research Chair program (950-228619 and 950-231990), the Canadian Foundation of Innovation (CFI 228619), Alberta Economic Development and Trade (grant RCP-14-022-SEG), and in part by CMC Microsystems. This material is based upon work supported by the U.S. National Science Foundation under grant 1636645.

References

[1] K. Jansky, "Directional studies of atmospherics at high frequencies," *Proc. Inst. Radio Eng.*, vol. 20, no. 12, pp. 1920–1932, Dec. 1932. doi: 10.1109/JRPROC.1932.227477.

[2] S. Okwit, "An historical view of the evolution of low-noise concepts and techniques," *IEEE Trans. Microw. Theory Techn.*, vol. 32, no. 9, pp. 1068–1082, Sept. 1984. doi: 10.1109/TMTT.1984.1132818.

[3] M. W. Pospieszalski, "Extremely low-noise amplification with cryogenic FETs and HFETs: 1970–2004," *IEEE Microw. Mag.*, vol. 6, no. 3, pp. 62–75, Sept. 2005. doi: 10.1109/MMW.2005.1511915.

[4] S. Weinreb, "Low-noise technology, 1982 state-of-the-art," in *Proc. IEEE Int. Microwave Symp.*, 1982, pp. 10–12.

[5] S. Weinreb, "Low-noise cooled GASFET amplifiers," *IEEE Trans. Microw. Theory Techn.*, vol. 28, no. 10, pp. 1041–1054, Oct. 1980.

[6] J. Schleeh et al., "Cryogenic LNAs for SKA band 2 to 5," in *Proc. IEEE MTT-S Int. Microw. Symp. (IMS)*, June 2017, pp. 164–167.

[7] A. Gerritsen and F. van den Burg, "The possibility for using an amplifier at low temperatures," *Physica*, vol. 17, no. 10, pp. 930–932, 1951. doi: 10.1016/0031-8914(51)90047-X.

[8] T. Nast and D. Murray, "Orbital cryogenic cooling of sensor systems," Aerospace Research Central, 1976. [Online]. Available: https://arc.aiaa.org/doi/abs/10.2514/6.1976-979.

[9] R. Ross, *Aerospace Coolers: A 50-Year Quest for Long-Life Cryogenic Cooling in Space*. New York: Springer New York, 2007, pp. 225–284.

[10] S. Weinreb and A. R. Kerr, "Cryogenic cooling of mixers for millimeter and centimeter wavelengths," *IEEE J. Solid-State Circuits*, vol. 8, no. 1, pp. 58–63, 1973. doi: 10.1109/JSSC.1973.1050345.

[11] G. Cortes-Medellin et al., "A fully cryogenic phased array camera radio astronomy," *IEEE Trans. Antennas Propag.*, vol. 63, no. 6, pp. 2471–2481, June 2015.

[12] L. Locke et al., "CryoPAF4: A cryogenic phased array feed design," in *Millimeter, Submillimeter, and Far-Infrared Detectors and Instrumentation for Astronomy VIII*, vol. 9914, W. S. Holland and J. Zmuidzinas, Eds., SPIE, July 2016, p. 99141P.

[13] P. K. Day, H. G. LeDuc, B. A. Mazn, A. Vayonakis, and J. Zmuidzinas, "A broadband superconducting detector suitable for use in large arrays," *Nature*, vol. 425, no. 6960, p. 817, 2003. doi: 10.1038/nature02037.

[14] M. Hosseini, W. Wong, and J. C. Bardin, "A 0.4–1.2 GHz SiGe cryogenic LNA for readout of MKID arrays," in *Proc. IEEE Int. Microw. Symp.*, Boston, June 2019, pp. 164–167.

[15] M. Klauda et al., "Superconductors and cryogenics for future communication systems," *IEEE Trans. Microw. Theory Techn.*, vol. 48, no. 7, pp. 1227–1239, 2000. doi: 10.1109/22.853466.

[16] J. C. Bardin et al., "A 28nm bulk-CMOS 4-to-8GHz ¡2mw cryogenic pulse modulator for scalable quantum computing," in *Proc. IEEE Int. Solid-State Circuits Conf.*, Feb. 2019, pp. 456–458.

[17] B. Patra et al., "Cryo-CMOS circuits and systems for quantum computing applications," *IEEE J. Solid-State Circuits*, vol. 53, no. 1, pp. 1–13, 2017. doi: 10.1109/JSSC.2017.2737549.

[18] B. Patra et al., "A scalable cryo-CMOS 2-to-20GHz digitally intensive controller for 4×32 frequency multiplexed spin qubits/transmons in 22nm FinFET technology for quantum computers," in *Proc. IEEE Int. Solid-State Circuits Conf.*, San Francisco, Feb. 2020, pp. 304–306.

[19] L. Le Guevel et al., "A 110mK 295µW 28nm FDSOI CMOS quantum integrated circuit with a 2.8GHz excitation and nA current sensing of an on-chip double quantum dot," in *Proc. IEEE Int. Solid-State Circ. Conf.*, San Francisco, Feb. 2020, pp. 306–307.

[20] S. Bonen et al., "Cryogenic characterization of 22-nm FDSOI CMOS technology for quantum computing ICs," *IEEE Electron Device Lett.*, vol. 40, no. 1, pp. 127–130, Jan. 2019.

[21] L. Belostotski, "Low-noise-amplifier (LNA) performance survey." Univ. of Calgary, Calgary, CA. [Online]. Available: https://schulich.ucalgary.ca/contacts/leo-belostotski

[22] L. Belostotski and J. W. Haslett, "Sub-0.2 dB noise figure wideband room-temperature CMOS LNA with non-50 Ω signal-source impedance," *IEEE J. Solid-State Circuits*, vol. 42, no. 11, pp. 2492–2502, 2007. doi: 10.1109/JSSC.2007.907172.

[23] L. Belostotski et al., "The first CMOS LNA on a radio telescope," in *Proc. Int. Symp. Antenna Technol. Appl. Electromagn.*, July 2014, pp. 1–3.

[24] A. J. Beaulieu, L. Belostotski, T. Burgess, B. Veidt, and J. W. Haslett, "Noise performance of a phased-array feed with CMOS low-noise amplifiers," *IEEE Antennas Wireless Propag. Lett.*, vol. 15, pp. 1719–1722, Feb. 2016. doi: 10.1109/LAWP.2016.2528818.

[25] T. Kulatunga, L. Belostotski, and J. W. Haslett, "400-to-800-MHz GaAs pHEMT-based wideband LNA for radio-astronomy antenna-array feed," *IEEE Microw. Compon. Lett.*, vol. 28, no. 10, pp. 909–911, Oct. 2018. doi: 10.1109/LMWC.2018.2864880.

[26] R. H. Witvers, J. G. B. de Vaate, and E. E. M. Woestenburg, "Sub 0.15dB noise figure room temperature GaAs LNA for next generation radio telescope," in *Proc. European Microw. Conf.*, Sept. 2010, pp. 1078–1081.

[27] J. Xu, W. A. Serdijn, B. Woestenburg, and J. G. bij de Vaate, "GaAs 0.5 dB NF dual-loop negative-feedback broadband low-noise amplifier IC," *Electron. Lett.*, vol. 41, no. 14, pp. 780–782, July 2005. doi: 10.1049/el:20051548.

[28] J. Schleeh, N. Wadefalk, P. A. Nilsson, and J. Grahn, "10 K room temperature LNA for SKA band 1," in *Proc. IEEE MTT-S Int. Microw. Symp. (IMS)*, May 2016, pp. 1–4. [Online]. Available: http://ieeexplore.ieee.org/document/7540344/

[29] S. Weinreb, R. Lai, N. Erickson, T. Gaier, and J. Wielgus, "W-band InP wideband MMIC LNA with 30 K noise temperature," in *Proc. IEEE MTT-S Int. Microw. Symp. Dig. (Cat. No.99CH36282)*, 1999, vol. 1, pp. 101–104.

[30] A. H. Akgiray et al., "Noise measurements discrete HEMT transistors application wideband very low-noise amplifiers, *IEEE Trans. Microw. Theory Techn.*, vol. 61, no. 9, pp. 3285–3297, Sept. 2013.

[31] S. Montazeri and J. C. Bardin, "A sub-milliwatt 4–8 GHz SiGe cryogenic low noise amplifier," in *Proc. IEEE Int. Microw. Symp. (IMS)*, June 2017, pp. 160–163.

[32] S. Weinreb, J. C. Bardin, and H. Mani, "Design of cryogenic SiGe low-noise amplifiers," *IEEE Trans. Microw. Theory Techn.*, vol. 55, no. 11, pp. 2306–2312, Nov. 2007. doi: 10.1109/TMTT.2007.907729.

[33] D. Loss and D. P. DiVincenzo, "Quantum computation with quantum dots," *Phys. Rev. A*, vol. 57, no. 1, pp. 120–126, Jan 1998. doi: 10.1103/PhysRevA.57.120.

[34] J. Koch et al., "Charge-insensitive qubit design derived from the Cooper pair box," *Phys. Rev. A*, vol. 76, no. 4, p. 042319, Oct. 2007. doi: 10.1103/PhysRevA.76.042319.

[35] F. Jazaeri, A. Beckers, A. Tajalli, and J. Sallese, "A review on quantum computing: From qubits to front-end electronics and cryogenic MOSFET physics," in *Proc. Int. Conf. Mixed Des. Integrated Circuits Syst.*, June 2019, pp. 15–25.

[36] A. Beckers, F. Jazaeri, and C. Enz, "Cryogenic MOS transistor model," *IEEE Trans. Electron Devices*, vol. 65, no. 9, pp. 3617–3625, Sept. 2018. doi: 10.1109/TED.2018.2854701.

[37] "IRE standards on methods of measuring noise in linear two-ports," *Proc. IRE*, vol. 48, no. 1, pp. 60–68, Jan. 1960. doi: 10.1109/JRPROC.1960.287380.

[38] M. W. Pospieszalski, "On the measurement of noise parameters of microwave two-ports," *IEEE Trans. Microw. Theory Techn.*, vol. 34, no. 4, pp. 456–458, 1986. doi: 10.1109/TMTT.1986.1133369.

[39] M. W. Pospieszalski et al., "Noise parameters and light sensitivity of low-noise high-electron-mobility transistors at 300 and 12.5 K," *IEEE Trans. Electron Devices*, vol. 33, no. 2, pp. 218–223, 1986. doi: 10.1109/T-ED.1986.22469.

[40] L. Escotte, F. Sejalon, and J. Graffeuil, "Noise parameter measurement of microwave transistors at cryogenic temperature," *IEEE Trans. Instrum. Meas.*, vol. 43, no. 4, pp. 536–543, 1994. doi: 10.1109/19.310165.

[41] J. Laskar, J. J. Bautista, M. Nishimoto, M. Hamai, and R. Lai, "Development of accurate on-wafer, cryogenic characterization techniques," *IEEE Trans. Microw. Theory Techn.*, vol. 44, no. 7, pp. 1178–1183, 1996. doi: 10.1109/22.508659.

[42] R. Hu and S. Weinreb, "A novel wide-band noise-parameter measurement method and its cryogenic application," *IEEE Trans. Microw. Theory Techn.*, vol. 52, no. 5, pp. 1498–1507, May 2004. doi: 10.1109/TMTT.2004.827029.

[43] I. Rolfes, T. Musch, and B. Schiek, "Cryogenic noise parameter measurements microwave devices," *IEEE Trans. Instrum. Measure.*, vol. 50, no. 2, pp. 373–376, Apr. 2001.

[44] W. Wiatr, "Comments on 'Cryogenic noise parameter measurements microwave devices'," *IEEE Trans. Instrum. Meas.*, vol. 53, no. 2, p. 619, Apr. 2004.

[45] D. Russell and S. Weinreb, "Cryogenic self-calibrating noise parameter measurement system," *IEEE Trans. Microw. Theory Techn.*, vol. 60, no. 5, pp. 1456–1467, 2012. doi: 10.1109/TMTT.2012.2188813.

[46] "Noise figure measurement accuracy – The Y-factor method," Agilent Technologies, Santa Rosa, CA, Application Note 57-2," Oct. 2004.

[47] J. Randa, E. Gerecht, D. Gu, and R. L. Billinger, "Precision measurement method cryogenic amplifier noise temperatures below 5 K," *IEEE Trans. Microw. Theory Techn.*, vol. 54, no. 3, pp. 1180–1189, Mar. 2006.

[48] J. E. Fernandez, "A noise-temperature measurement system using a cryogenic attenuator," Telecommun. Mission Operations Progress Rep., July 1998.

[49] L. Belostotski, "On the number of noise parameters for analyses of circuits with MOSFETs," *IEEE Trans. Microw. Theory Techn.*, vol. 59, no. 4, pp. 877–881, Apr. 2011. doi: 10.1109/TMTT.2011.2109734.

[50] R. Q. Lane, "The determination of device noise parameters," *Proc. IEEE*, vol. 57, no. 8, pp. 1461–1462, Aug. 1969. doi: 10.1109/PROC.1969.7311.

[51] M. Mitama and H. Katoh, "An improved computational method noise parameter measurement," *IEEE Trans. Microw. Theory Techn.*, vol. 27, no. 6, pp. 612–615, June 1979.

[52] A. Boudiaf, M. LaPorte, J. Dangla, and G. Vernet, "Accuracy improvements in two-port noise parameter extraction method," in *Proc. IEEE Int. Microw. Symp.*, Albuquerque, NM, June 1–5, 1992, pp. 1569–1572.

[53] L. Escotte, R. Plana, and J. Graffeuil, "Evaluation noise parameter extraction methods," *IEEE Trans. Microw. Theory Techn.*, vol. 41, no. 3, pp. 382–387, Mar. 1993. doi: 10.1109/22.223735.

[54] L. Belostotski and J. W. Haslett, "Evaluation tuner-based noise-parameter extraction methods very low noise amplifiers," *IEEE Trans. Microw. Theory Techn.*, vol. 58, no. 1, pp. 236–250, Jan. 2010. doi: 10.1109/TMTT.2009.2036411.

[55] M. Himmelfarb and L. Belostotski, "On impedance-pattern selection for noise parameter measurement," *IEEE Trans. Microw. Theory Techn.*, vol. 64, no. 1, pp. 258–270, Jan. 2016. doi: 10.1109/TMTT.2015.2504500.

[56] A. T. Sutinjo and L. Belostotski, "Analytical determinant of the noise parameter extraction matrix and its applications," in *Proc. USNC-URSI Radio Sci. Meeting (Joint AP-S Symp.)*, July 2019, pp. 81–82.

[57] M. De Dominicis, F. Giannini, E. Limiti, and G. Saggio, "A novel impedance pattern fast noise measurements," *IEEE Trans. Instrum. Measure.*, vol. 51, no. 3, pp. 560–564, June 2002. doi: 10.1109/TIM.2002.1017728.

[58] S. Van den Bosch and L. Martens, "Improved impedance-pattern generation for automatic noise-parameter determination," *IEEE Trans. Microw. Theory Techn.*, vol. 46, no. 11, pp. 1673–1678, Nov. 1998. doi: 10.1109/22.734556.

[59] A. T. Sutinjo, L. Belostotski, B. Juswardy, and D. X. C. Ung, "A measure of well-spread points in noise wave-based source matrix for wideband noise parameter measurement: The SKA-Low example," *IEEE Trans. Microw. Theory Techn.*, vol. 68, no. 5, pp. 1783–1793, 2020. doi: 10.1109/TMTT.2020.2977287.

[60] S. Colangeli, Cleriti, W. Ciccognani, and E. Limiti, "Evaluation of coaxial cable performance under thermal gradients," *Int. J. Microw. Wirel. Tech.*, vol. 7, nos. 3–4, pp. 239–249, 2015. doi: 10.1017/S1759078715000069.

[61] M. W. Pospieszalski, "Modeling of noise parameters of MESFETs and MODFETs and their frequency and temperature dependence," *IEEE Trans. Microw. Theory Techn.*, vol. 37, no. 9, pp. 1340–1350, 1989. doi: 10.1109/22.32217.

[62] A. Sheldon, L. Belostotski, G. Messier, and A. Madanayake, "Impact of noise bandwidth on noise figure," *IEEE Trans. Instrum. Meas.*, vol. 68, no. 7, pp. 2662–2664, July 2019. doi: 10.1109/TIM.2019.2900145.

[63] NoiseTech Microwaves Ltd., "Wideband noise parameter measurements at hot and cryogenic temperatures," *Microw. J.*, June 2018. [Online]. Available: https://www.microwavejournal.com/articles/30493-wideband-noise-parameter-measurements-at-hot-and-cryogenic-temperatures

[64] "Keysight 2-port and 4-port PNA-X network analyzer," Agilent Technologies, Santa Rosa, CA.

[65] "Smart noise sources SNS series: Operating and service guide (N4000A, N4001A, and N4002A)," Agilent Technologies, Santa Rosa, CA.

[66] J. Randa, "Noise-parameter uncertainties: A Monte Carlo simulation," *J. Res. Nat. Inst. Standards Technol.*, vol. 107, no. 5, pp. 431–444, Sept. 2002. doi: 10.6028/jres.107.037.

[67] A. Sheldon, L. Belostotski, H. Mani, C. E. Groppi, and K. F. Warnick, "Automated noise-parameter measurements of cryogenic LNAs," in *Proc. IEEE ARFTG Microwave Measurement Conference (ARFTG)*, 2021, to be published.